Int. J. Electrochem. Sci., 16 **(2021)** 151011, doi: 10.20964/2021.01.18

International Journal of
ELECTROCHEMICAL
SCIENCE
www.electrochemsci.org

Effect of Calcining Temperatures on the Electrochemical Performances of $LiNi_{0.5}Co_{0.2}Mn_{0.3}O_2$ Cathode Material for Lithium Ion Batteries

Xiaoman Wang, Hai-Lang Zhang[*]

School of Chemical and Material Engineering, Jiangnan University, Wuxi Jiangsu 214122, China
[*]E-mail: zhl8868@vip.163.com

Received: 16 September 2020 / *Accepted:* 25 October 2020 / *Published:* 30 November 2020

In this paper, the effects of calcination temperatures on the electrochemical properties of $LiNi_{0.5}Co_{0.2}Mn_{0.3}O_2$ cathode materials for lithium ion batteries were studied. The $LiNi_{0.5}Co_{0.2}Mn_{0.3}O_2$ materials were prepared by a sol-gel method at 750 ºC, 800 ºC, 850 ºC and 900 ºC, respectively. In order to study the effects of calcination temperatures on the material, X-ray diffraction, scanning electron microscope, charge/discharge cycle test, cyclic voltammetry test and impedance test were used to characterize and test the materials. The results show that with the increase of calcination temperature, the particles of $LiNi_{0.5}Co_{0.2}Mn_{0.3}O_2$ materials change from spherical to regular polyhedron. The $LiNi_{0.5}Co_{0.2}Mn_{0.3}O_2$ material prepared at higher calcination temperature has better electrochemical properties, but too high calcination temperature will also have adverse effects on the properties of the materials. When the calcination temperature is 850 ºC, the particle size of $LiNi_{0.5}Co_{0.2}Mn_{0.3}O_2$ material is uniform with good dispersion, high crystallinity and good layered structure. And also it has the best electrochemical performance. The first discharge specific capacity of the material prepared at this calcination temperature is 168.3mAh g^{-1} with a retention rate is 90.4% after 50 cycles.

Keywords: Li-ion battery, calcining temperature, $LiNi_{0.5}Co_{0.2}Mn_{0.3}O_2$, sol-gel method, electrochemical performance

1. INTRODUCTION

As one advanced power supply, secondary lithium-ion battery has the advantages of high energy density, high working voltage, long cycle life, no memory effect, low self-discharge and low environmental pollution. It has been widely used in portable electronic products such as mobile phones, laptops and digital cameras [1-2]. In modern society, lithium-ion batteries are being developed for application in the field of power batteries and energy storage batteries. So hiher energy density and long cycle life would be required.

As an important part of lithium-ion battery, cathode material largely determines the performance of lithium-ion battery, and its development is very important for the development of lithium-ion battery [3-4]. The $LiFePO_4$ cathode material with olivine structure[5] and $LiCoO_2$ with layered structure[6-8] are the most commonly used cathode materials in lithium ion batteries. $LiFePO_4$ has the disadvantages of low theoretical capacity, low electrical conductivity, poor rate performance and poor cycling performance. $LiCoO_2$ has the disadvantages of high cost, poor stability and high toxicity. In recent years, $Li[Ni_xCo_yMn_{1-x-y}]O_2$ ternary cathode materials have been found to have more advantages[9]. The ternary cathode materials with layered structure have employed the advantages of $LiCoO_2$, $LiNiO_2$ and $LiMnO_2$ with high capacity and low production cost. They are considered as one of the promising lithium ion cathode materials in the lithium battery industry[9-11]. In $Li[Ni_xCo_yMn_{1-x-y}]O_2$ ternary cathode materials, nickel element is the main active materials of electrode materials to improve the capacity of materials, cobalt element can effectively improve the conductivity and rate performance of materials, and manganese element has good electrochemical inertia which can make the material maintain a stable structure[12-13]. $Li[Ni_xCo_yMn_{1-x-y}]O_2$ cathode material has a layered structure of α-$NaFeO_2$ and belongs to R-3m space group, which is similar to the hexagonal system of $LiCoO_2$. Li occupiy the 3a site of space group, O occupy 6c site and the transition metal atoms are surrounded by six oxygen atoms to form a MO_6 octahedral structure, which is randomly located in the 3b site of the transition metal layer[14-15]. Relatively, $LiNi_{1/3}Co_{1/3}Mn_{1/3}O_2$ (NCM111) and $LiNi_{0.4}Co_{0.2}Mn_{0.4}O_2$ (NCM442) have been studied with more publicatons for a longer time[9]. Only in recent years, $LiNi_{0.5}Co_{0.2}Mn_{0.3}O_2$ (NCM532) cathode material has become a research hotspot due to its higher discharge specific capacity, good cycle stability, low cost and environmental friendliness[16]. So NCM532 cathode material has been paid more attention in our laboratory.

The preparation conditions of ternary cathode materials, such as calcination time, calcination temperature and excess lithium content, may affect the lattice structure, particle morphology and electrochemical performance of the materials[17]. Among these factors, especially the calcination temperature could be the most synthesis condition. So in this study, $LiNi_{0.5}Co_{0.2}Mn_{0.3}O_2$ cathode materials have been prepared by sol-gel method at different calcination temperatures to find the optimum calcination temperature. The effects of calcination temperatures on the structure and electrochemicalproperties of ternary cathode materials have been systematically investigated.

2. EXPERIMENTAL

2.1. Preparation of materials

According to stoichiometric ratio, weighed proper amounts of the $LiNO_3$(99%%), $Ni(NO_3)_2$•$6H_2O$(A.R grade), $Co(NO_3)_2$•$6H_2O$(A.R grade), $Mn(CH_3COO)_2$•$4H_2O$(A.R grade) and citric acid(A.R grade),respectively. The summation of the moles of metal salts is equal to the mole of citric acid. Then dissolved them in deionized water respectively. Mixing the dissolved solutions in a clean beaker, stirring evenly, and adjusted the pH value to 7-8 with concentrated ammonia water. The mixture was heated in a water bath at a constant temperature 80 ^oC, stirring at the same time with a stirrer to

evaporate the water until the gel was formed. The gel was placed in a drying box and dried at 120 ^{o}C for 24 h. The gel was pre-sintered at 600 ^{o}C for 6h, and then cooled to room temperature. Then calcined it at 750 ^{o}C high temperature in air atmosphere for 21 h, , and then cooled to room temperature. After grinding, $LiNi_{0.5}Co_{0.2}Mn_{0.3}O_2$ material was obtained. With the same way, another three samples were prepared at 800 ^{o}C, 850 ^{o}C and 900 ^{o}C, respectively.

2.2. Material characterization

The D8 advanced X-ray diffractometer was used to conduct X-ray diffraction (XRD) test on the samples to explore the crystal characteristics of the prepared materials. XRD tests were carried out with Cu target Ka radiation at 30 kV tube voltage with 25 mA tube current. The scan data were in the 2θ range from 10^{o} to 90^{o} in step of 4^{o}/min. The morphology of the samples was observed by S-4800 cold field emission scanning electron microscope. Noran System Six X-ray energy spectrometer was used for qualitative and quantitative analysis of the element composition of the samples.

2.3. Electrochemical measurement

Electrochemical experiments were performed using two-electrode [9]. The fabrication process for the CR2032 type coin cells was similar to that in our previous publication[9]. The electrode was prepared by mixing active material, acetylene black and polyvinylidene fluoride (PVDF) at the mass ratio of 80:12:8. Acetylene black was used as conductive agent and PVDF as binder. PVDF was dissolved in 1-methyl-2-pyrrolidone (NMP) before mixing the three raw materials. After grinding the mixture into a uniform paste, the paste is coated on the aluminum foil with a Doctor blade technique, then pressed at 10MPa and dried at 100 *°C* for 12 h in a vacuum oven, and then it was punched into a certain size disc as the positive electrode. Then it was punched into a certain size disc as the positive electrode. The CR2032 coin cells were assembled in an argon-filled glove box (SUPER 1220/750, made in Shanghai, China), using lithium metal as the counter electrode, Celgard 2325 as the separator, and 1 M LiPF6 in 1:1 EC:DMC solution as the electrolyte. At room temperature, constant current charge and discharge tests were carried out in a voltage range of 3.0-4.4 V and at a current density of 0.1C by LAND battery test system (Wuhan, China). The cyclic voltammetry (CV) was measured at a scanning rate of 0.1 mv s^{-1} in the voltage range of 2.5-4.6V by IM6 electrochemical workstation (Made in Germany). The electrochemical impedance spectroscopy (EIS) experiment was carried out in the frequency range of 100kHz to 10MHz and at the amplitude of 10 mV.

3. RESULTS AND DISCUSSION

3.1. Crystal structure analysis

Figure 1 shows the XRD patterns of $LiNi_{0.5}Co_{0.2}Mn_{0.3}O_2$ cathode materials obtained by calcination at different temperatures. It can be seen from the figure that the four cathode materials belong

to the standard layer structure of α-$NaFeO_2$ with the space group of R-3m. For ternary materials, the ionic radius of Ni^{2+} is close to that of Li^+, which leads to cation mixing. The structure information of the crystal can be known by XRD, and the degree of Li^+/Ni^{2+} mixing for ternary cathode materials can be known. In the analysis of XRD spectra, it is generally believed that when the ratio of peak value of *I(003)* and *I(104)* (*R* value) was more than 1.2 and the peak position of group (006)/(012) and (018)/(110) show obvious splitting state, the degree of Li^+/Ni^{2+} mixing degree should be lower[18]. Table 1 shows the lattice parameters of $LiNi_{0.4}Co_{0.2}Mn_{0.4}O_{2-x}Cl_x$ cathode materials. When *c/a* is above 4.89 , the material would have a good layered structure[19].

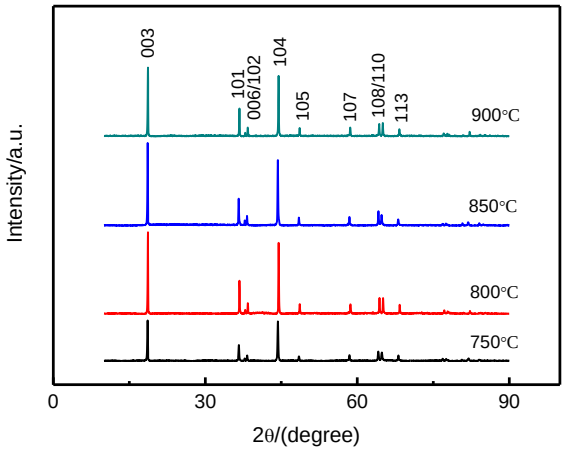

Figure 1. XRD patterns of the $LiNi_{0.5}Co_{0.2}Mn_{0.3}O_2$ calcined at different temperatures.

Table 1. Lattice parameters of the $LiNi_{0.5}Co_{0.2}Mn_{0.3}O_2$ calcined at different temperatures

Temperature	*a*/nm	*c*/nm	*c/a*	I_{003}/I_{104}	*V*/Å^3
750 °C	2.8668	14.2285	4.9632	1.122	101.10
800 °C	2.8614	14.2253	4.9713	1.251	101.23
850 °C	2.8632	14.2377	4.9726	1.274	101.87
900 °C	2.8627	14.2421	4.9749	1.193	100.98

For the material with the calcination temperature of 750 °C , as shown in Table 1, the XRD peak value I_{003}/I_{104} of the material is small. From Figure 1 , it could be seen that the peak shape is very weak, and even a little impurity peak appears. The splitting of (006)/(012) and (018)/(110) peak is not obvious, and the ratio of (003) and (104) peak is 1.12. The reason may be that when the calcination temperature is too low, the diffusion rate of atoms or ions in the solid phase is slower, so the reaction rate is slower, the reaction is not sufficient and it is not easy to form high crystallinity materials. With the increase of calcination temperature, the diffraction peak intensity of the material is also relatively increased, the splitting of (006)/(102) and (018)/(110) peaks becomes wider.The *R* value is also relatively increased,

c/a value also increases. It shows that the degree of cation mixing decreases when the sintering temperature is above 800 °C , and the layered structure of the material developes better. When the calcination temperature is 900 °C, the *R* value decreases to a certain extent, which indicates that the mixing of cations is intensified, which may be caused by the serious volatilization of lithium salt caused by too high temperature[20].

3.2. Morphology analysis

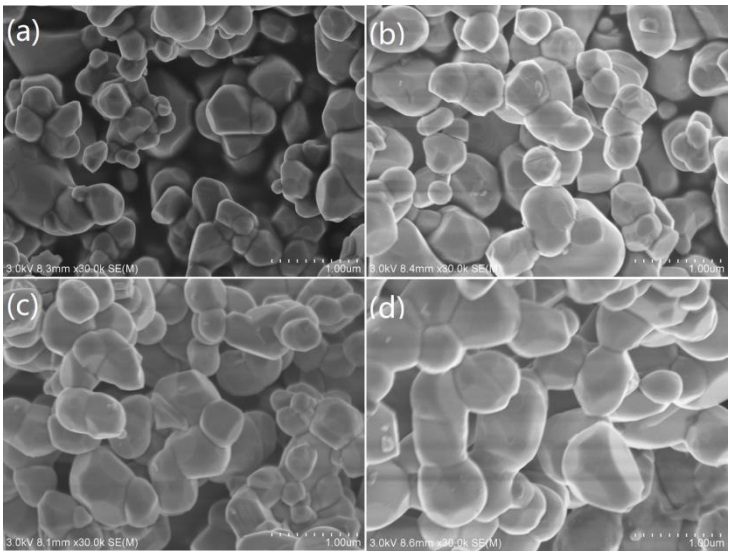

Figure 2. SEM images of the $LiNi_{0.5}Co_{0.2}Mn_{0.3}O_2$ calcined at different temperatures.

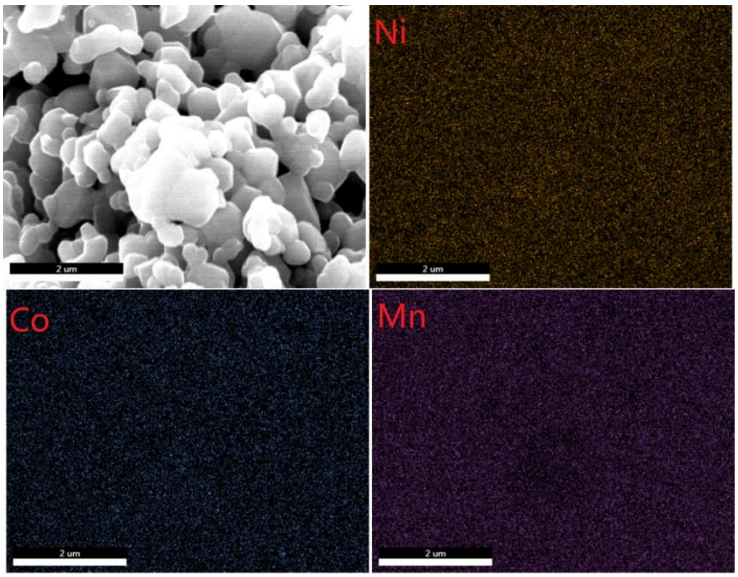

Figure 3. EDS diagram of the $LiNi_{0.5}Co_{0.2}Mn_{0.3}O_2$ calcined at 850 °C.

Figure 2 shows the SEM images of the samples at different calcination temperatures. It can be seen from the figure that the surface morphology of $LiNi_{0.5}Co_{0.2}Mn_{0.3}O_2$ powders synthesized at different

temperatures have obvious difference. The primary particles of the cathode materials synthesized at 750 °C did not grow up obviously. Combining with the XRD results, it was speculated that the calcination temperature was too low to provide enough diffusion power for the solid-state reaction. With the increase of calcination temperature, the primary particle size becomes larger, which is consistent with the XRD results that the crystallinity of the material is getting better with the increase of calcination temperature. As shown in Figure 2(d), when the sintering temperature is increased to 900 °C , the primary particles have grown obviously, but the samples sintered at this temperature show obvious hardening phenomenon and form large heterogeneous particles. This may lead to the electrolyte not fully infiltrate the electrode surface, resulting in the difficulty of detachment and embedding for Li^+ [21], thus affecting the charge and discharge performance of the material. When the calcination temperature is 850 °C , the dispersion of the particles is good and the agglomeration phenomenon is weakened. Only some large particles appear. The average particle size of the material is less than 0.5μm, the surface of the particles is smooth and the edges are clear, indicating that the crystallinity of the material is good. The results show that the samples sintered at 850 °C have better microstructure.

Figure 3 shows the EDS diagram of $LiNi_{0.5}Co_{0.2}Mn_{0.3}O_2$ cathode material calcined at 850 °C. From the EDS element distribution diagram, we can clearly see the existence of Ni, Co and Mn elements. The depth of color and the density of points in the figure represent the distribution content of each element. It can be seen that the distribution shape of each element is consistent and evenly distributed in the sample. This indicates that $LiNi_{0.5}Co_{0.2}Mn_{0.3}O_2$ cathode material with uniform distribution of various elements can be prepared by sol-gel method at 850 °C.

3.3. Electrochemical characterization

Figure 4 shows the constant current charge and discharge performance of $LiNi_{0.5}Co_{0.2}Mn_{0.3}O_2$ cathode material prepared at 750 °C, 800 °C, 850 °C, 900 °C for the initial cycle in the voltage range of 3-4.4 V and at current density of 0.1C. It can be seen that when the calcination temperature rises from 750 °C to 900 °C , the first discharge specific capacity increases first and then decreases. As shown in the figure, at 0.1C rate, the $LiNi_{0.5}Co_{0.2}Mn_{0.3}O_2$ cathode materials calcined at the four temperatures have a discharge platform at about 3.8 V. The first discharge specific capacities of the four samples are 146.6 mAh g^{-1}, 158.5mAh g^{-1}, 168.3mAh g^{-1}, and 152.4mAh g^{-1},respectively. Obviously, the first discharge specific capacity of the material calcined at 850°C shows the best electrochemical performance, which is corresponding to the good crystallinity and low cation mixing of the samples calcined at 850°C.

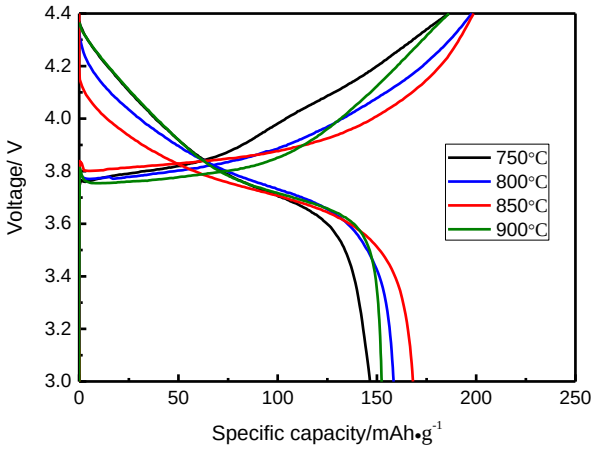

Figure 4. Initial charge and discharge curves of the $LiNi_{0.5}Co_{0.2}Mn_{0.3}O_2$ calcined at different temperatures.

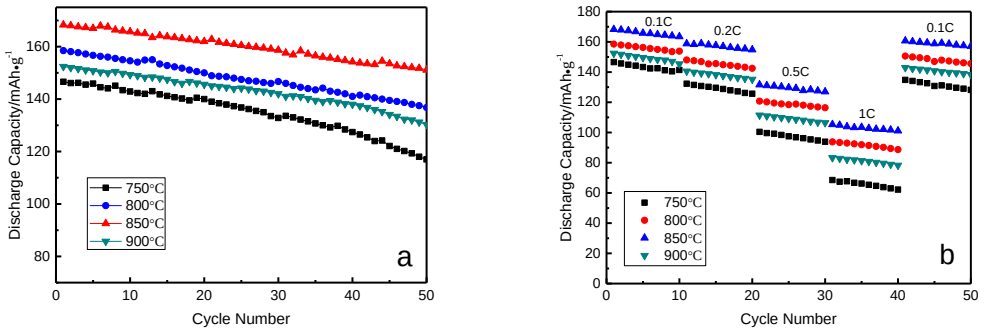

Figure 5. Cycle performances (a) and rate capability (b) of the $LiNi_{0.5}Co_{0.2}Mn_{0.3}O_2$ materials calcined at different temperatures.

Figure 5(a) shows the cycle performance of $LiNi_{0.5}Co_{0.2}Mn_{0.3}O_2$ cathode materials prepared at 750 °C, 800 °C, 850 °C , 900 °C for 50 cycles in the voltage range of 3-4.4 V and at current density of 0.1C. The results show that the a cathode material synthesized at 850 °C has relatively stable cycle performance. The capacity retention rate is 90.4% after 50 cycles at 0.1C rate, which is better than 87.3% of the cathode material prepared at 800 °C. The cyclic stability of the cathode materials synthesized at 750 °C and 900 °C is poor. After 50 cycles, their capacity retention rates are 80.5% and 84.7%, respectively. At 750 °C , it is possible that the solid-state sintering reaction does not have enough energy to promote the crystal growth, and the lattice development is incomplete, which leads to the blocking of ion diffusion and poor electrochemical performance. When the calcination temperature reaches 950 °C , the excessive volatilization of lithium salt and the reduction of Ni^{3+} may lead to poor electrochemical performanc[22]. In conclusion, the $LiNi_{0.5}Co_{0.2}Mn_{0.3}O_2$ cathode material prepared at 850 °C has thw best cycle performance.

Figure 5(b) shows the rate capability of $LiNi_{0.5}Co_{0.2}Mn_{0.3}O_2$ cathode materials prepared at 750 °C , 800 °C , 850 °C , 900 °C (cycling at 0.1C, 0.2C, 0.5C, 1.0C and 0.1C for 10 cycles for each rate,

respectively). It can be seen that the discharge specific capacity of the prepared materials at different temperatures decreased to different degrees at different current densities. Compared with the materials prepared at 800 °C and 850 °C , the discharge specific capacity of the materials prepared at 750 °C and 900 °C decreased significantly faster, especially at the high rate of 0.5C and 1C. At the initial rate of 0.1C, the discharge specific capacities of the materials prepared at 750 °C , 800 °C, 850 °C and 900 °C, respectively, did not differ much. At 1C rate, the discharge specific capacities of the materials prepared at the four temperatures are 68.5 mAh g^{-1}, 93.8 mAh g^{-1}, 105.3 mAh g^{-1} and 83.3 mAh g^{-1}, respectively. The obvious capacity difference is larger, while the specific capacity of the materials prepared at 850 °C is higher. When the rate returns to 0.1C, the specific capacity of the material prepared at 850 °C is closer to the data of the first circle to show an excellent rate capability.

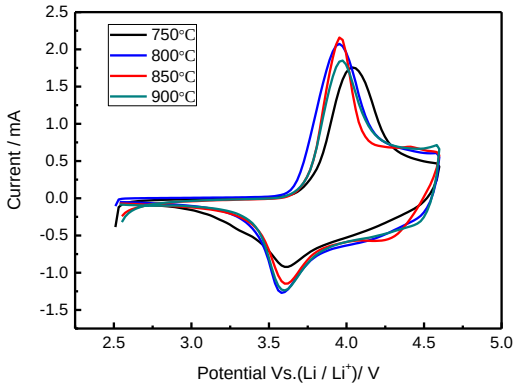

Figure 6. Cyclic voltammetry of the $LiNi_{0.5}Co_{0.2}Mn_{0.3}O_2$ materials calcined at different temperatures in the first cycle.

Figure 6 shows the cyclic voltammetry of $LiNi_{0.5}Co_{0.2}Mn_{0.3}O_2$ cathode materials prepared at 750 °C , 800 °C , 850 °C , and 900 °C, respectively, in the first cycle at a scanning rate of 0.1 mV s^{-1} and in the voltage range of 2.5-4.6 . As shown in the figure, the shapes of the four test curves are similar, showing clear oxidation and reduction peaks. These two peaks are considered as the oxidation/reduction reaction of Ni^{2+}/Ni^{4+} and Co^{3+}/Co^{4+} [23], accompanied by the process of detachment and embedding for Li^+. There is no red-ox peak at about 3V, which indicates that there is no manganese enriched spinel phase in the circulation process. The results show that the oxidation peak and reduction peak for $LiNi_{0.5}Co_{0.2}Mn_{0.3}O_2$ cathode material prepared at 850 °C is 3.954V and 3.602V, respectively, and the potential difference is 0.352V. The oxidation peaks of the cathode materials calcined at 750 °C , 800 °C and 900 °C shifted to higher voltage with potential differences of 0.436 V, 0.373 V and 0.361 V, respectively. The cathode material calcined at 850 °C has the smallest potential difference, which indicates that the polarization degree of the battery is small. So the cathode material calcined at 850 °C has better crystallinity, the irreversible phase change of material phase structure is small, and the reversibility of de-intercalation and intercalation for Li^+ is better.

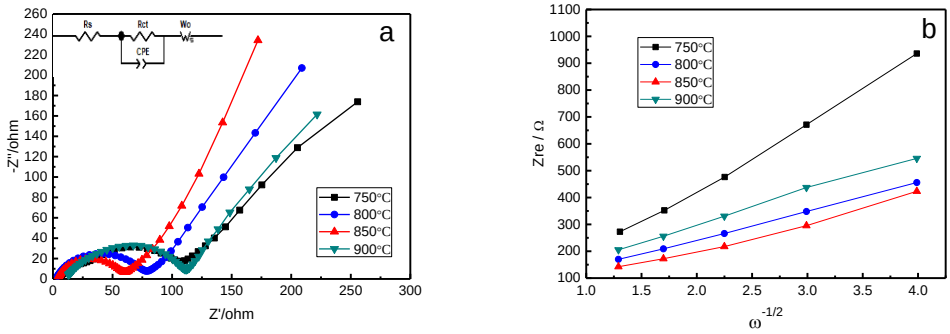

Figure 7. (a) EIS plots and (b) corresponding relationship between Z_{re} and $\sigma\omega^{-1/2}$ of the the $LiNi_{0.5}Co_{0.2}Mn_{0.3}O_2$ calcined at different temperatures in the first cycle.

Table 2. Impedance Data of he the $LiNi_{0.5}Co_{0.2}Mn_{0.3}O_2$ calcined at different temperatures in the first cycle.

Temperature	R_s	R_{ct}	σ	D_{Li+}(cm^2 s^{-1})
750 °C	2.32	132.50	249.41	1.91×10^{-14}
800 °C	2.36	79.11	106.05	9.74×10^{-14}
850 °C	3.75	57.63	97.71	1.27×10^{-13}
900 °C	10.12	107.10	128.21	7.23×10^{-14}

Figure 7. (a) and (b) shows the AC impedance characteristics at the test frequency of 100kHz to 10MHz and the corresponding relationship between Z_{re} and $\sigma\omega^{-1/2}$ of $LiNi_{0.5}Co_{0.2}Mn_{0.3}O_2$ cathode materials prepared at 750 °C , 800 °C , 850 °C and 900 °C, respectively, in the first cycle. The AC impedance characteristic diagram consists of a semicircle in high frequency region and an oblique line. The semicircle in the high frequency region is related to the internal charge transfer impedance (R_{ct}). The oblique line in the low frequency region represents the Warburg diffusion impedance of lithium ion in the cathode material, and the distance from the origin to the first intersection point of the semicircle and the abscissa represents the ohmic impedance (R_s) of the solution. The EIS curve was fitted by Zview software, and the calculated impedance value and lithium ion diffusion coefficient (D_{Li+}) were shown in Table 2. It can be seen that the R_{ct} of the cathode material prepared at 850 °C is smaller, which is 57.63 Ω. At this calcination temperature, the D_{Li+} of the material is relatively large, which is 1.27×10^{-13} cm^2 s^{-1}. The results show that when the calcination temperature is 850 °C , the charge transfer impedance of the material is the minimum, and the transfer of Li^+ is easier, which is consistent with the high specific capacity and high cycle performance.

4. CONCLUSIONS

By comparing the XRD images of $LiNi_{0.5}Co_{0.2}Mn_{0.3}O_2$ materials synthesized at four calcination temperatures 750 °C , 800 °C , 850 °C and 900 °C , respectively, it is found that with the increase of temperature, the diffraction peak becomes sharper, the crystallinity degree increases, and the degree of cation mixing decreases. However, when the temperature is too high, the layered structure of the material will be destroyed. Through the SEM images of calcined samples, it can be seen that the higher the temperature, the closer the particles are combined, the smoother the surface of the particles, and the particle size will gradually increase. When the temperature rises to 900 °C , the particle size increases obviously, accompanied with the hardening phenomenon, which makes the capacity of the material decrease. Furthermore, the comparison of the electrochemical performance of the battery made of four different materials at different temperatures also shows that the battery made of $LiNi_{0.5}Co_{0.2}Mn_{0.3}O_2$ cathode material calcined at 850 °C has the best charge and discharge performance. The first discharge specific capacity is 168.3 mAh g^{-1}. After 50 cycles, the specific capacity remains 152.1 mAh g^{-1}, and the retention rate is 90.4%.

References

1. J. B. Goodenough，K. Park, *J. Am. Chem. Soc*., 135 (2013) 1167.
2. G. Zubi, R. Dufo-López, M. Carvalho, G. Pasaoglu, Renewable and Sustainable Energy Reviews, 89 (2018)292.
3. J. B. Goodenough, A. Manthiram, *MRS Communications*, 4 (2014) 135.
4. D. Andre, S.J. Kim, P. Lamp, S. F. Lux, F. Maglia, O. Paschos, B. Stiaszny, *J. Mater. Chem. A*, 3 (2015) 6709.
5. B. Scrosati, G. Jürgen, *J. Power Sources*, 195 (2010) 2419.
6. E. Antolini, *Solid State Ionics*, 170(2004) 159.
7. M. S. Whittingham, *Chem. Rev*. 104 (2004) 4271.
8. T. Ohzuku, A. Ueda, *J. Electrochem. Soc*., 141 (1994) 2677.
9. H. L. Zhang, F. J. Wu, *Int. J. Electrochem. Sci.*, 15 (2020) 7417.
10. Y. K. Lei, J. J. Ai, S. Yang, C. Y. Lai, Q. J. Xu, *J. Taiwan Institute of Chemical Engineers*, 97(2019) 255.
11. K. C. Wu, F. Wang, L. L. Gao, M. R. Li, L. L. Xiao, L. T. Zhao, S. J. Hu, X. J. Wang, Z. L. Xu, Q. G. Wu, *Electrochim.Acta*, 75 (2012) 393.
12. Y. Chen, G. X. Wang, K. Konstantinov, H. K. Liu, S. X. Dou, *J. Power Sources*, 119 (2003) 184.
13. Y. Koyama, I. Tanaka, H. Adachi, Y. Makimura, T. Ohzuku, *J. Power Sources*, 119 (2003) 644.
14. M. Oishi, T. Fujimoto, Y. Takanashi, Y. Orikasa, *J. Power Sources*, 222 (2013) 45.
15. P. Y. Liao, J. G. Duh, S. R. Sheenb, *J. Electrochem. Soc*., 152 (2005) A1695.
16. S.Y. Yang, X.Y. Wang, X. K. Yang, Y. S. Bai, Z. L. Liu, H. B. Shu, Q. L. Wei, *Electrochim. Acta*, 66 (2012) 88.
17. A. Kaufmann, G. H. Frischat, *Solid State Ionics*,105 (1998) 297.
18. S. K. Martha, H. Sclara, Z. S. Framowitz, D. Kovacheva, N. Saliyski, Y. Gofer, P. Sharon, E. Golik, B. Markovsky, D. Aurbach, *J. Power Sources*, 189 (2009) 248.
19. Y. K. Sun, S. T. Myung, B. C. Park, K. Amine, *Chem. Mater*., 18 (2006) 5159.
20. A. Iqbal, D. Li, *Chem. Phys. Letters*, 720 (2019) 97.
21. S. H. Wu, C. W. Yang, J. Power Sources, 146 (2005) 270.
22. D. Versaci, R. Nasi, U. Zubair, J. Amici, M. Sgroi, M. A. Dumitrescu, C. Francia, S. Bodoardo , N.

Penazzi, *J. Solid State Electrochem.*, 21 (2017) 3429.
23. J. Fu, D. Mu, B. Wu, J. Bi, X. Liu, Y. Peng, Y. Li, F. Wu, *Electrochim. Acta*, 246 (2017) 27.
24. Y. K. Sun, S. W. Cho, S. W. Lee, C. S. Yooh, K. Amine, *J. Electrochem. Soc.*, 154 (2006) A168.